



## Enhanced exciton separation through negative energy band bending at grain boundaries of Cu<sub>2</sub>ZnSnSe<sub>4</sub> thin-films

A. R. Jeong, W. Jo, S. Jung, J. Gwak, and J. H. Yun

Citation: [Applied Physics Letters](#) **99**, 082103 (2011); doi: 10.1063/1.3626848

View online: <http://dx.doi.org/10.1063/1.3626848>

View Table of Contents: <http://scitation.aip.org/content/aip/journal/apl/99/8?ver=pdfcov>

Published by the [AIP Publishing](#)

---

### Articles you may be interested in

[Atom probe tomography study of internal interfaces in Cu<sub>2</sub>ZnSnSe<sub>4</sub> thin-films](#)

J. Appl. Phys. **118**, 095302 (2015); 10.1063/1.4929874

[Defect chemistry and chalcogen diffusion in thin-film Cu<sub>2</sub>ZnSnSe<sub>4</sub> materials](#)

J. Appl. Phys. **117**, 074902 (2015); 10.1063/1.4907951

[Microstructural analysis of 9.7% efficient Cu<sub>2</sub>ZnSnSe<sub>4</sub> thin film solar cells](#)

Appl. Phys. Lett. **105**, 183903 (2014); 10.1063/1.4901401

[Fabrication of polycrystalline Cu<sub>2</sub>ZnSnSe<sub>4</sub> layers with strongly preferential grain orientation via selenization of Sn/Cu/ZnSe\(001\)/GaAs\(001\) structures](#)

Appl. Phys. Lett. **104**, 071913 (2014); 10.1063/1.4866436

[Optical properties of high quality Cu<sub>2</sub>ZnSnSe<sub>4</sub> thin films](#)

Appl. Phys. Lett. **99**, 062104 (2011); 10.1063/1.3624827

---

The image shows the cover of an Applied Physics Reviews journal issue. It features a blue and orange color scheme with a molecular structure background. The text 'NEW Special Topic Sections' is prominently displayed in white. Below it, the text 'NOW ONLINE' is in yellow, followed by 'Lithium Niobate Properties and Applications: Reviews of Emerging Trends' in white. The AIP Applied Physics Reviews logo is in the bottom right corner.

## NEW Special Topic Sections

**NOW ONLINE**  
Lithium Niobate Properties and Applications:  
Reviews of Emerging Trends

**AIP** Applied Physics  
Reviews

# Enhanced exciton separation through negative energy band bending at grain boundaries of $\text{Cu}_2\text{ZnSnSe}_4$ thin-films

A. R. Jeong,<sup>1</sup> W. Jo,<sup>1,a)</sup> S. Jung,<sup>2</sup> J. Gwak,<sup>2</sup> and J. H. Yun<sup>2</sup>

<sup>1</sup>Department of Physics, Ewha Womans University, Seoul 120-750, South Korea

<sup>2</sup>Photovoltaic Research Center, Korea Institute of Energy Research, Daejeon 305-343, South Korea

(Received 4 June 2011; accepted 29 July 2011; published online 23 August 2011)

Local surface potential of  $\text{Cu}_2\text{ZnSnSe}_4$  thin-films was investigated by Kelvin probe force microscopy. The surface potential profile across grain boundaries (GBs) shows a rise of 200–600 meV at GBs in a Cu-poor and Zn-poor film with 3.8% efficiency, which means positively charged GBs. In contrast, the GBs in a Cu-poor and Zn-rich film with 2% efficiency exhibit lowering of surface potential by 40 meV. The results indicate that GBs of  $\text{Cu}_2\text{ZnSnSe}_4$  films play a role for exciton separation and governing defects for high efficiency could be not only  $\text{Cu}_{\text{Zn}}$  but also  $\text{V}_{\text{Cu}}$  as explained theoretical predictions. © 2011 American Institute of Physics. [doi:10.1063/1.3626848]

$\text{Cu}_2\text{ZnSnSe}_4$  (CZTSe) has received significant interest since they show high absorption coefficient ( $>10^4 \text{ cm}^{-1}$ ) and contains only earth abundant and non-toxic elements of Cu, Zn, Sn, and Se.<sup>1–4</sup> CZTSe thin-films have been fabricated by a variety of processes,<sup>1–5</sup> which have been recorded the best conversion efficiency as high as 9.3% by a chemical method. However, the efficiency of CZTSe thin-films fabricated by a vacuum process is vexingly so far achieved as 3.2%.<sup>6</sup> In order to increase the efficiency of CZTSe solar films, it is critical to understand the carrier transport as well as to develop a proper process condition.

For  $\text{Cu}(\text{In,Ga})\text{Se}_2$  (CIGS) photovoltaic films,<sup>7</sup> it is known that the electron-hole recombination reduces at grain boundaries (GBs) confirmed by Kelvin probe force microscopy (KPFM) measurement.<sup>8,9</sup> KPFM measurements yield the electrostatic properties of GBs and determine the band bending across GBs.<sup>9</sup> In this letter, we evaluate the surface potential across GBs with respect to composition and conversion efficiency.

CZTSe thin-films were deposited on Mo/soda lime glass substrates by co-evaporating Cu, Zn, Sn, and Se using Kundsens-type effusion films as evaporation sources at base pressure of  $5 \times 10^{-6}$  Torr. The KPFM measurements were carried out in a commercial atomic force microscopy (AFM) (Nanofocus Inc., n-Tracer) with a Pt/Ir coated cantilever. Topography was measured in a contact mode, followed by measurement of surface potential. The surface potential was determined under a non-contact mode by applying AC voltage with amplitude of 1.0 V and frequency of 70 kHz. The scanning rate and size were controlled with 0.5 Hz and  $2.0 \mu\text{m}$  to minimize topological artifacts. X-ray diffraction (XRD), energy dispersive spectrometry (EDS), and Auger electron spectroscopy (AES) were used to examine the structural and compositional properties as well.

Figure 1(a) shows XRD patterns of the CZTSe thin-films. The peaks in the reflections indicate that the films are polycrystalline and the reflections are identified with crystallographic planes such as (112), (220)/(224), and (116)/(312) of the kesterite  $\text{Cu}_2\text{ZnSnSe}_4$ . The lattice parameters are

determined  $a = 5.67 \pm 0.01 \text{ \AA}$  and  $c = 11.34 \pm 0.05 \text{ \AA}$ , which are in good agreement with reported values.<sup>10–12</sup>

Table I indicates photovoltaic parameters of the samples. Thickness of the CZTSe layers is  $2.6 \mu\text{m}$ . Low conversion efficiency was observed in the film (1), which has relatively poor  $J_{sc}$ . It is notable that the open circuit voltage is not much different over the samples. The film (1) indicating low conversion efficiency and poor  $J_{sc}$  shows small grain size, which are less than  $1 \mu\text{m}$  as shown in Fig. 1(b). For the films with improved conversion efficiency, considerable grain growth was observed in Figs. 1(c) and 1(d). As CIGS thin-films, it is required to increase both carrier diffusion length and built-in potential in polycrystalline thin-film absorbers since it is known to be effective for exciton separation.<sup>13,14</sup>

Depth-profile distributions for the films are shown in Fig. 2. This quantitative assessment indicates different depth profiles, especially Zn and Sn elements. It reveals a uniform distribution in film (1), while Zn is increased toward the interface and Sn exhibits a broad peak in the middle of films (2) and (3). The different elemental distributions due to the process would be one of the strong reasons for improving photovoltaic film characteristics, which is also supported by the EDS results as shown in Table II.

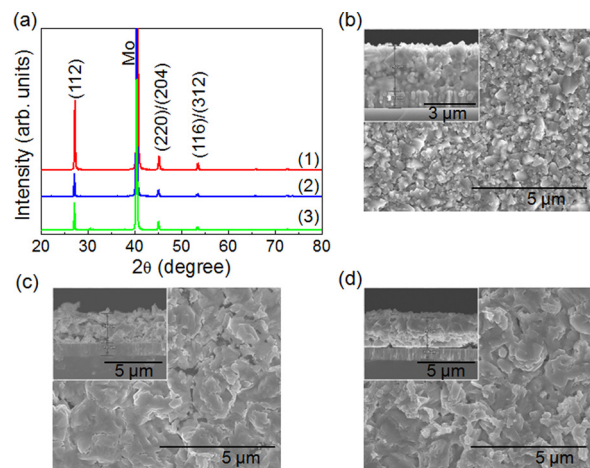


FIG. 1. (Color online) (a) XRD patterns of CZTSe thin-films deposited by co-evaporation. (b)–(d) Plane view of SEM micrographs of CZTSe thin-films. The insets show the cross-sectional view of the samples with  $2.6 \mu\text{m}$  of thickness.

<sup>a)</sup>Electronic mail: wjjo@ewha.ac.kr. Tel.: +82-2-3277-4066.

TABLE I. Efficiency ( $\eta$ ), open-circuit voltage ( $V_{oc}$ ), short-circuit current ( $J_{sc}$ ), and fill factor ( $F.F.$ ) of the samples obtained from  $I$ - $V$  measurement.

Sample No.	Thickness ( $\mu\text{m}$ )	Eff. (%)	$V_{oc}$ (V)	$J_{sc}$ (mA/cm <sup>2</sup> )	$F.F.$
(1)	2.62	2.08	0.229	18.4	0.494
(2)	2.59	3.17	0.302	31.4	0.335
(3)	2.62	3.82	0.272	36.8	0.382

In Figure 3, the surface potential of grains and their GBs was compared with images of the topography, in which the bright region indicates high potential. In Figs. 3(a)–3(c), topography, surface potential, and line profile for the film (1) are displayed for clarifying behaviors between grain interior (GI) and GBs. This result explains the negatively charged GBs with a positive energy band bending tend to favor recombination around GBs. As already discussed, the small grains of the film (1) are main causes for low conversion efficiency. In addition, the band bending at GBs might be another source of inferiority. Consequently, the negative potential at GBs of the film (1) reduces the conversion efficiency, which is resulted from reduced  $J_{sc}$ .

In Figs. 3(d)–3(i), topography and surface potential are shown for the samples over 3% of conversion efficiency. In one-dimensional line scans across GBs, the films (2) and (3) exhibit larger surface potential values than the film (1) due to a considerable increase of potential near GBs. A positive surface potential of Figs. 3(e) and 3(h) at GBs are designated by line profiles in Figs. 3(f) and 3(i). This observation supports the idea that positively charged GBs repel holes and attract electrons, which should help exciton separation and suppress recombination as shown in Fig. 4(b), which is very promising for high efficiency films like CIGS.<sup>8,13,15</sup>

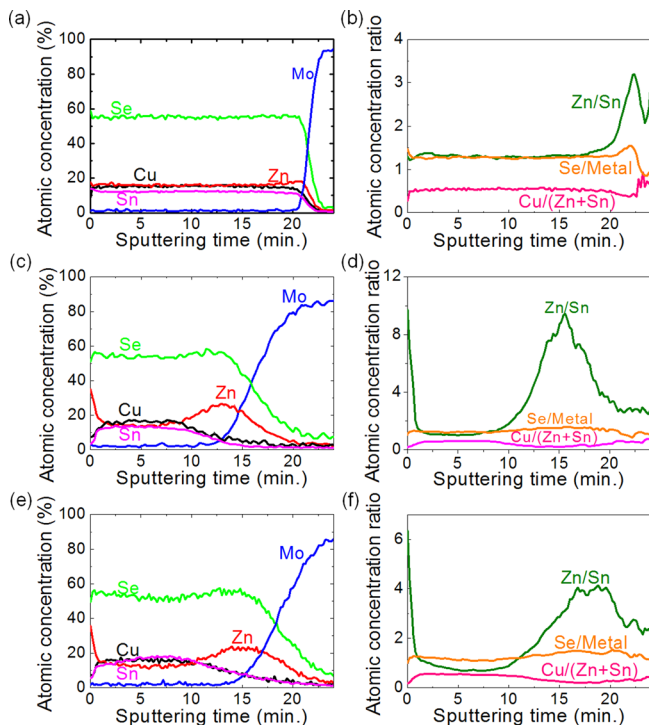


FIG. 2. (Color online) (a), (c), (e) Depth profile of CZTSe of (a) the films (1)–(3) by Auger electron spectroscopy, respectively. (b), (d), (f) Relative atomic ratio through the CZTSe films.

TABLE II. Chemical composition of the CZTSe thin-films probed by EDS measurement.

Sample No.	Cu	Zn	Sn	Se	Cu/(Zn + Sn)	Zn/Sn
(1)	22.68	18.81	11.35	47.16	0.75	1.65
(2)	22.87	24.74	13.55	41.84	0.64	1.60
(3)	21.06	16.36	18.90	43.68	0.59	0.86

For a ternary compound  $\text{CuInSe}_2$ , the dominant  $p$ -type acceptor defect is the Cu vacancy ( $V_{\text{Cu}}$ ).<sup>16,17</sup> However, in the quaternary materials related to CZTSe, the formation energy of neutral  $V_{\text{Cu}}$  is much larger than  $\text{Cu}_{\text{Zn}}$ .<sup>18</sup> Our local electrical results also imply alternative dominant defects in accordance with thin-film contents. The films are nearly stoichiometric with Cu-poor and Zn-rich, as the film (3) has Zn-poor contents. A theoretical prediction validates that the equilibrium growth condition (Cu-rich and Zn-poor) is required to form the high quality CZTSe samples, where  $\text{Cu}_{\text{Zn}}$  will dominate over  $V_{\text{Cu}}$ .<sup>19</sup> The film (3) with Zn-poor contents measured by our EDS analysis slightly improved efficiency of 3.82% than those of film (2) with 3.17% being Cu-poor and Zn-rich. We suggest that formation of the other dominant defect such as  $\text{Cu}_{\text{Zn}}$  should help to enhance the photovoltaic film efficiency since  $\text{Cu}_{\text{Zn}}$  can form the Zn-poor film (3) easier than the Zn-rich film (2). But, a good photovoltaic film has been known as Cu-poor and Zn-rich condition,<sup>4,19,20</sup> which has the effect of enhancing the formation of  $V_{\text{Cu}}$  and suppressing the formation of  $\text{Cu}_{\text{Zn}}$ . In our case of the film (3), Zn content is higher near the surface from AES, which could lead to form  $V_{\text{Cu}}$  easily at the surface.

Figure 5 indicates maximum surface potential distribution from the number of events in the KPFM images. The shift to negative direction of the efficiency is increased. Defect states from the relative composition ratio explains maximum surface potential shift due to the change of dominant acceptor defect whether  $V_{\text{Cu}}$  or  $\text{Cu}_{\text{Zn}}$ .<sup>20</sup>

$$E_F - E_V = kT \ln \frac{N_V}{N_A}, \quad (1)$$

where  $E_F$  and  $E_V$  are Fermi energy level and valence band maximum,  $k$  is Boltzmann's constant and  $T$  is the absolute temperature,  $N_V$  is the effective density of state of valence band, and  $N_A$  is the acceptor impurity density, respectively,

$$N_A^- = \frac{N_A}{1 + \frac{1}{g} \exp\left(\frac{E_A - E_F}{kT}\right)}, \quad (2)$$

where  $N_A^-$  is the ionized acceptor, and  $g$  is the ground state degeneracy for acceptor levels.<sup>21</sup> From Eqs. (1) and (2), Fermi energy shift, depending on the  $N_A$ , is changed by  $E_A - E_F$  due to the different defects. The calculated acceptor transition energy level for  $V_{\text{Cu}}$  is at 0.02 eV above the VBM, whereas the level for  $\text{Cu}_{\text{Zn}}$  is at 0.10 eV above the VBM, thus the acceptor level of  $V_{\text{Cu}}$  is shallow.<sup>22</sup> The result also proves existence of other dominant defects of  $\text{Cu}_{\text{Zn}}$ .

In summary, the significant positive enhancement of surface potential at the GBs would contribute to improve of the photovoltaic film efficiency. Local electrical

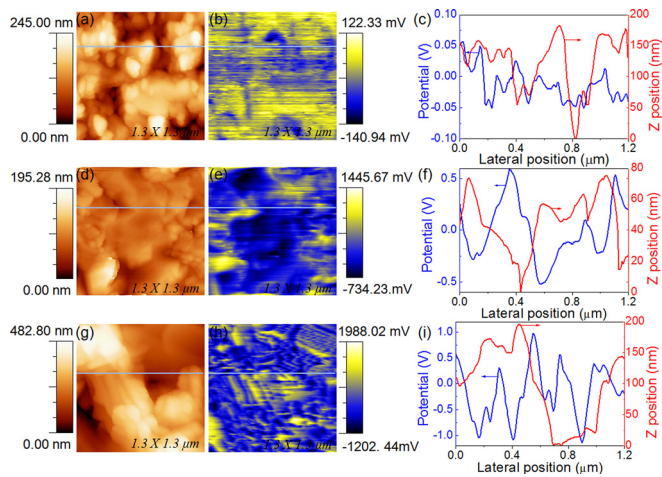


FIG. 3. (Color online) (a), (d), (g) Topographic images of surfaces of the CZTSe and (b), (e), (h) their corresponding KPFM images. (c), (f), (i) One-dimensional potential and topography line profiles. The film (1) with 2.08% of conversion efficiency show negative potential, while films (2) and (3) has positive potential.

measurement shows positive potential at GBs, which leads to the negative energy band bending where the holes are repelled. The change of local electrical properties is indicated depending on the composition of CZTSe, especially Cu/(Zn + Sn) and Zn/Sn. Although the optimal growth condition is controversial,  $\text{Cu}_{\text{Zn}}$  as well as  $V_{\text{Cu}}$  could be a strong candidate for the dominant acceptor.

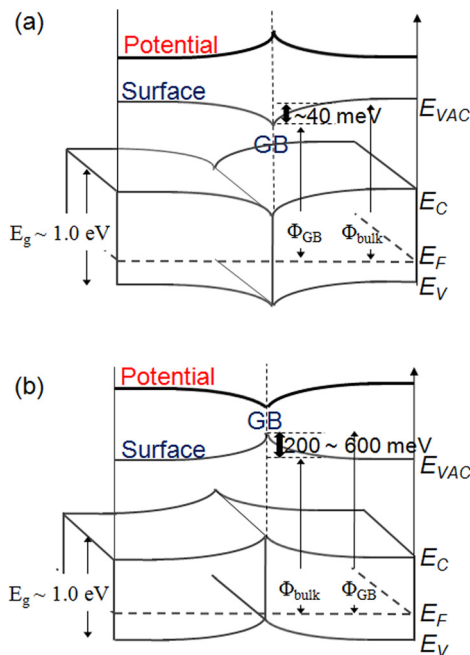


FIG. 4. (Color online) Illustration of the energy band diagram across a GB in (a) the film (1) with 2% of conversion efficiency and (b) the films (2) and (3) with over 3% of conversion efficiency of the CZTSe films. According to the KPFM measurements, the work function  $\Phi_{\text{GB}}$  at the GB is negative in the film (1). The opposite accounts for the films (2) and (3).

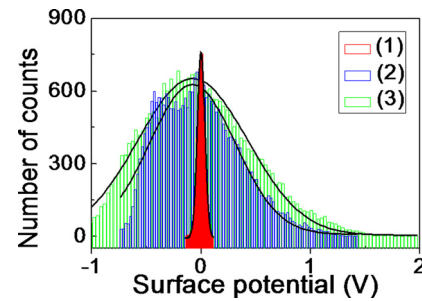


FIG. 5. (Color online) Surface potential distribution of the films (1)–(3).

This research was supported by a grant from the Fundamental R&D Program for Core Technology of Materials funded by the Ministry of Knowledge Economy, Republic of Korea (No. 10037233), by KRCF (Korea Research Council of Fundamental Science & Technology), and KIER (Korea Institute of Energy Research) for “NAP (National Agenda Project) program.” This work was supported in part by MEST and DGIST (10-BD-0101, Convergence Technology with New Renewable Energy and Intelligent Robot).

- <sup>1</sup>K. Wang, O. Gunawan, T. Todorov, B. Shin, S. J. Chey, N. A. Bojarczuk, D. Mitzi, and S. Guha, *Appl. Phys. Lett.* **97**, 143508 (2010).
- <sup>2</sup>B.-A. Schubert, B. Marsen, S. Cinque, T. Unold, R. Klenk, S. Schorr, and H.-W. Schock, *Prog. Photovoltaics* **19**, 93 (2011).
- <sup>3</sup>H. Katagiri, K. Jimbo, S. Yamada, T. Kamimura, W. S. Maw, T. Fukano, T. Ito, and T. Motohiro, *Appl. Phys. Express* **1**, 041201 (2008).
- <sup>4</sup>A. Ennaoui, M. Lux-Steiner, A. Weber, D. Abou-Ras, I. Kötschau, H.-W. Schock, R. Schurr, A. Hölzing, S. Jost, and R. Hock, *Thin Solid Films* **517**, 2511 (2009).
- <sup>5</sup>T. K. Todorov, K. B. Reuter, and D. B. Mitzi, *Adv. Mater.* **22**, E156 (2010).
- <sup>6</sup>G. Zoppi, I. Forbes, R. W. Miles, P. J. Dale, J. J. Scragg, and L. M. Peter, *Prog. Photovoltaics* **17**, 315 (2009).
- <sup>7</sup>M. A. Green, K. Emery, Y. Hishikawa, and W. Warta, *Prog. Photovoltaics* **19**, 84 (2011).
- <sup>8</sup>Y. Yan, C.-S. Jiang, R. Noufi, S.-H. Wei, H. R. Moutinho, and M. M. Al-Jassim, *Phys. Rev. Lett.* **99**, 235504 (2007).
- <sup>9</sup>G. Hanna, T. Glatzel, S. Sadewasser, N. Ott, H. P. Strunk, U. Rau, and J. H. Werner, *Appl. Phys. A* **82**, 1 (2006).
- <sup>10</sup>Y. Yan, R. Noufi, and M. M. Al-Jassim, *Phys. Rev. Lett.* **96**, 205501 (2006).
- <sup>11</sup>S. Siebentritt, S. Sadewasser, M. Wimmer, C. Leendertz, T. Eisenbarth, and M. Ch. Lux-Steiner, *Phys. Rev. Lett.* **97**, 146601 (2006).
- <sup>12</sup>C. Persson and A. Zunger, *Phys. Rev. Lett.* **91**, 26 (2003).
- <sup>13</sup>M. J. Hetzer, Y. M. Strzhemechny, M. Gao, M. A. Contreras, A. Zunger, and L. J. Brillson, *Appl. Phys. Lett.* **86**, 162105 (2005).
- <sup>14</sup>A. Bosio, N. Romeo, A. Podesta, S. Mazzamuto, and V. Canevari, *Crystr. Res. Technol.* **40**, 1048 (2005).
- <sup>15</sup>H. Mönig, Y. Smith, R. Caballero, C. A. Kaufmann, I. Laueremann, M. Ch. Lux-Steiner, and S. Sadewasser, *Phys. Rev. Lett.* **105**, 116802 (2010).
- <sup>16</sup>S. B. Zhang, S.-H. Wei, A. Zunger, and H. Katayama-Yoshida, *Phys. Rev. B* **57**, 9642 (1998).
- <sup>17</sup>J. M. Raulot, C. Domain, and J. F. Guillemoles, *J. Phys. Chem. Solids* **66**, 2019 (2005).
- <sup>18</sup>D. S. Albus, J. J. Carapella, J. R. Tuttle, and R. Noufi, *Mater. Res. Soc. Symp. Proc.* **228**, 267 (1991).
- <sup>19</sup>S. Chen, X. G. Gong, A. Walsh, and S.-H. Wei, *Appl. Phys. Lett.* **96**, 021902 (2009).
- <sup>20</sup>C. Persson, *J. Appl. Phys.* **107**, 053710 (2010).
- <sup>21</sup>S. M. Sze, *Physics of Semiconductor Devices* (John Wiley & Sons, Inc. New York, 1969).
- <sup>22</sup>S. Chen, A. Walsh, Y. Luo, J.-H. Yang, X. G. Gong, and S.-H. Wei, *Phys. Rev. B* **82**, 195203 (2010).